Flexible Multilayer Combining Nickel Nanowires and Polymer Films for Broadband Microwave Absorption

Yann Danlée, Christian Bailly, Isabelle Huynen, *Senior Member, IEEE*, and Luc Piraux

***Abstract*—In front of electromagnetic (EM) pollution of the environment, EM protection requires more and more efficient solutions. Multilayered films consisting of alternating stacked nickel nanowires (NWs)-based conductive layers separated by bulk polycarbonate films were fabricated as thin electromagnetic shield. The well-defined periodic arrangement of the multilayer structure with gradient NW concentration in the conductive layers demonstrates a remarkably high effective microwave absorption (reflection and transmission below −10 dB, up to 34.3 dB of absorption loss) by tuning the conductivity and magnetic permeability of each layer. The ferromagnetic nature of NWs enhances the absorption performances compared to nonmagnetic carbon nanotubes having similar conductivity. Our method provides a simple, compact, and efficient approach for the fabrication of electromagnetic interference shielding materials offering improved broadband microwave absorption.**

***Index Terms*—Nanomaterials, radar absorbing materials, shielding modeling and methods.**

I. Introduction

In THE present urban, domestic, and working place environments, electromagnetic (EM) waves are omnipresent. The major trends toward ever wideband wireless communication, on one hand, and ever increasing density of electronic devices, on the other hand, generate a growing issue with electromagnetic interference (EMI), which can occur between devices or between subcomponents of devices. The consequences are at best disturbing but can be very dangerous for health- or security-related applications [1]. Classical broadband EMI shielding is based on electromagnetic reflectors, usually metal foils or coatings, acting as Faraday cages [2]. These methods are less and less satisfactory in the present environment because the interfering EM signal is simply reflected back to the environment without significant loss. This explains the renewed popularity of EM absorbers, which truly eliminate the EM signal in directions or locations where it is unwanted.

To reach effective EM absorption, a delicate balance between the complex permittivity and permeability must be achieved [3]. In short, the EM properties of the material must minimize transmission and reflection. The transmission is defined as

$$T = e^{\frac{-i\omega d}{c}\sqrt{\varepsilon_r \mu_r}} \tag{1}$$

where d is the thickness of material, ω is the pulsation, and c is the speed of light in vacuum. The imaginary part of permittivity ε_r and permeability μ_r must by high to decrease the transmission. Moreover, the complex values of those two physical properties must be close to each other to minimize the reflection coefficient at material/air interface defined by [4]

$$R = \frac{\sqrt{\frac{\mu_r}{\varepsilon_r}} - 1}{\sqrt{\frac{\mu_r}{\varepsilon_r}} + 1}. \tag{2}$$

Polymer-based nanocomposites containing conductive and ferromagnetic fillers can fulfill these contradictory demands [5]–[8]. As conductive fillers, carbon nanotubes (CNTs) [9] or metallic nanowires (NWs) [10] are attractive choices because of their extremely high intrinsic conductivity. CNTs are widely used because the percolation threshold can be reached at low loading owing to their easy dispersibility in selected polymers [11]. The low permittivity matrix, on the other hand, allows EM waves to penetrate deeply in the absorbing structure, while the conducting network dissipates the EM energy through complex resistive–capacitive coupling and multiple internal reflections [12]. The nonmagnetic nature of CNTs limits their attenuating influence only to the electric field of the EM wave, while conducting ferromagnetic particles also dissipate the magnetic field as the wave penetrates the material. The combination of conductivity and magnetism drastically amplify the energy absorption [6], [8]. In this context, new types of high-performance absorbers have emerged. Among the most common nanocomposite build from the ferromagnetic component in polymer, we have the dispersion of magnetic NWs [6], [13], [14], the use of grafted magnetic nanoparticles (MNPs) on carbonaceous nanostructures [15], [16] or even the elaboration of ferromagnetic particles trapped inside CNTs [17], [18]. The NWs incorporation gets sufficiently high magnetic permeability and well-balanced conductivity to yield a significant absorption enhancement. We select then the very efficient combination of

Manuscript received May 20, 2019; revised August 19, 2019; accepted September 13, 2019. Date of publication October 15, 2019; date of current version October 13, 2020. This work was supported by the National Fund for Scientific Research (F.R.S.-FNRS) and Fonds pour la formation à la Recherche dans l'Industrie et dans l'Agriculture (FRIA). *(Corresponding author: Yann Danlée.)*

Y. Danlée is with the Institute of Information and Communication Technologies, Electronics and Applied Mathematics, Université catholique de Louvain, 1348 Louvain-la-Neuve, Belgium, and also with the Institute of Condensed Matter and Nanosciences, Université catholique de Louvain, 1348 Louvain-la-Neuve, Belgium (e-mail: yann.danlee@uclouvain.be).

C. Bailly and L. Piraux are with the Institute of Condensed Matter and Nanosciences, Université catholique de Louvain, 1348 Louvain-la-Neuve, Belgium (e-mail: christian.bailly@uclouvain.be; luc.piraux@uclouvain.be).

I. Huynen is with the Institute of Information and Communication Technologies, Electronics and Applied Mathematics, Université catholique de Louvain, 1348 Louvain-la-Neuve, Belgium (e-mail: isabelle.huynen@uclouvain.be).

Color versions of one or more of the figures in this article are available online at http://ieeexplore.ieee.org.

Digital Object Identifier 10.1109/TEMC.2019.2943549

polymer and Ni-NWs as the building blocks of our broadband microwave absorber.

In addition to the intrinsic properties of the material, the arrangement of layers plays an important role in the absorption process. A gradual increase in conductivity and/or magnetic permeability allows impedance matching at the incoming wave front [19]. Reflection is lower and the wave propagates deeper into the material where the energy is "trapped" between the internal lossy layers with less outside reflection [3], [20]. Gradient structure, hence, leads to a higher overall absorption due to reduced reflected power.

This article presents novel hierarchically organized multilayers built from micrometer deposition of a network of nickel nanowires (Ni-NWs) on polymer films, which are very effective EM absorbers in the microwave frequency range. The structures are obtained by alternatively stacking conductive-ferromagnetic and insulating layers. The effectiveness of the multilayers is linked to the gradient periodic arrangement of the ferromagnetic depositions, which enhances impedance matching. The structures are easy to make, very thin (thickness much lower than the centimeter wavelength), and conformable. Moreover, the multilayers proposed in this article are modular (easy restacking to reach another absorption target).

II. Materials and Methods

A. Ni-NWs and Sandwiches

Although not so widely available as CNTs, ferromagnetic NWs have the potential advantage to combine high electrical conductivity with enhanced magnetic property. This is the case for Ni-NWs that combine large aspect ratio, high conductivity, and high magnetic permeability. Amongst ferromagnetic materials, nickel has a strong magnetic susceptibility ($\chi = 110$) and offers a cheap and facile implementation. Nanoparticles are very sensitive to oxidation, yet nickel owns advantageous resistance to oxidation unlike particles of iron [15], [21]. Ni-NWs appear as ideal candidates as subcomponents of optimal absorbing multilayers. We synthesize Ni-NWs by electrodeposition inside the pores of a nanoporous alumina template. The selected membranes, UniKera Standard from IDT Inc. (Synkera), provide a very homogeneous distribution of pores. The pore areal density is up to 35%, a sufficient density for small-scale production. The diameter of the pores is 150 nm and the membrane is 100 μm thick; the geometry of the pores obviously defines the shape of the NWs. The NW growth starts from the cathode that is directly deposited on the membrane. For this purpose, a 20 nm chromium layer is first evaporated by e-beam (Pfeiffer Vacuum Classic 500 supplied by Intellemetrics IL150) on one side of the membrane to make a strong interface between alumina and the actual cathode. Next, 1000 nm copper is evaporated as the cathode on the Cr interface layer. The opposite side of the template is free to let the electrolytic solution flow into the pores. The electrodeposition of pure Ni-NWs is done from a solution of boric acid (H_3BO_3) 0.6M and nickel sulfate hexahydrate ($NiSO_4 \cdot 6H_2O$) 0.5M mixed at room temperature. The potentiostat (model 263 A from EG&G Princeton Applied Research) measures the current flow between the working and counter electrodes; the total charge is used to estimate the mass of electrodeposited material inside the porous membrane. Additional details about the process are given in [22].

The aim of the electrodeposition process is to obtain a large amount of NWs. Once synthesized, the NWs have to be extracted from alumina. First, the cathode is completely etched away. Copper is etched in 0.5M $FeCl_3$ for 3–4 min. Afterwards, chromium is etched in 2–3 min by a caustic solution of 0.33M $KMnO_4$ and 5M NaOH. At this stage, the NWs are still strongly embedded in the membrane. The set is dived in 8M NaOH heated at 70 °C for 24 h. During the last minutes, ultrasonication is applied to ensure a good separation of the residual cluster of Ni-NWs. The suspension of NWs is quickly filtered with the help of a polycarbonate ipPORE Track Etched Membrane from it4ip (25 μm-thick porous film with a pore density of 5×10^8 cm^{-2} and a pore diameter of 200 nm). The NWs are collected on the polymer filter. Acetic acid (50%) is directly passed through the filter in order to neutralize potential residues of NaOH on the polymer and the surface of the NWs. Let us note that the exposure time to NaOH, and then, acetic acid is insufficient to affect strongly the polymer properties. Next, the NWs are rinsed with pure water, and finally, dried in an oven for 24 h at 120 °C.

The entangled NWs already form a thin mesh on the filter. To facilitate handling, the covered filter is directly sandwiched between two 55 μm-thick Lexan polycarbonate (PC) films. The sandwich is hot pressed at 210 °C, 10 T for 30 s. The fabrication of the magnetic multilayer is schematized in Fig. 1. This process has the advantage of simplicity and yields confined thin conductive magnetic films.

This article has studied a sandwich built from four layers having a density of Ni-NWs of 0.29, 0.47, 0.92, and 3.26 mg/cm^2 (over a fixed surface of 950 mm^2). The average thickness of NW depositions is about 7 μm and a single sandwich is 125 μm thick. The characterization is performed in the next section on each film in order to establish their effective EM response.

B. Magnetic and Electromagnetic Characterizations

The magnetization curves of the films were obtained using an alternating gradient field magnetometer (AGFM) instrument from Lake Shore with a maximum applied field of ±10 kOe. The B- and H-fields are measured before saturation where the static permeability is computed by the equation: $\mu_s = \frac{B}{H.\mu_o}$.

The frequency response of the samples is characterized using a Keysight N5247 A PNA-X vector network analyzer (VNA) operating up to 67 GHz. Physical properties (e.g., dielectric constant, conductivity, and permeability) are calculated from S-parameters provided by the instrument. We used the method of Nicolson and Ross [23] that has been completed by Weir [24]. This method is the most adapted for medium conductive and/or magnetic materials. For broadband measurements with moderate resolution, the method has a potential accuracy of about $\hat{A} \pm 0.1$ dB and $\hat{A} \pm 1\hat{A}^\circ$ with a significant reduction in mismatch errors [23]. Furthermore, the algorithm uses the Kramers–Kronig relations to ensure the uniqueness of the solution [25]. The algorithm provides physical properties with the right sign from S-parameters. The in-plane parameters are obtained from a waveguide configuration. The wave propagation in the direction

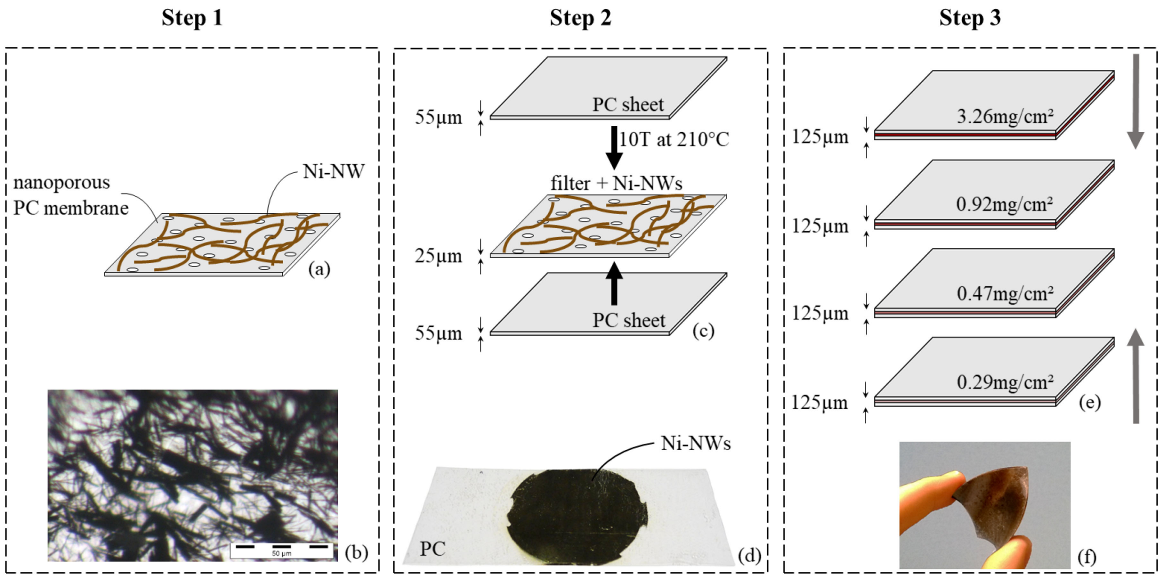

Fig. 1. Illustration of the fabrication of Ni-NWs-based multilayer. (a) Ni-NWs are collected on the nanoporous polycarbonate filter. (b) Optical image of entangled NWs over the filter surface. (c) Filter with the Ni-NWs is sandwiched between two polycarbonate sheets. (d) Photo of a single sandwich, the entangled Ni-NWs appear in black. (e) Sandwiches are stacked in gradient of concentration of Ni-NWs. (f) Photo of the multilayer.

perpendicular to the film (out-of-plane) corresponds to the microstrip configuration; the measurement needs then to connect a test fixture Anritsu 3680v equipment to the VNA. The techniques are explained and illustrated in [26].

The EM characterization is requisite to assess the physical properties of each film independently. Next, a homemade MATLAB routine simulates the output parameters (reflectance, transmittance, absorbance) of the multilayer based on the measurement of each single film. Each layer is treated like a transmission line with associated characteristic impedance Z_c and propagation constant γ. The layers are assumed isotropic in the three spatial dimensions. 50Ω impedances are placed on each side ports to account for the internal reference impedance of the VNA [27]. This method is used to display the theoretical prediction in the graphs of measurement. Moreover, an optimization by convergence with the MATLAB function $fmincon$ allows to quickly determine the local optimal stack of the layers in terms of input parameters (i.e., permittivity, permeability, thickness, and number of layers) [28].

A common way to quantify the performance of an absorber is the shielding effectiveness (SE) as the logarithmic ratio of the incident power P_i to outgoing power P_o of radiation. It can be expressed as the sum of reflection, absorption, and rereflection losses

$$\mathrm{SE} = 10\log_{10}\frac{P_i}{P_o} = \mathrm{SE}_A + \mathrm{SE}_R + \mathrm{SE}_M \qquad (3)$$

where SE_A, SE_R, and SE_M are absorption loss, reflection loss, and multiple reflection loss, respectively [29], [30]. This approach primarily aims to minimize transmission, or in other terms, favors absorption as well as reflection [29]. Focusing on absorption only, we prefer working with the absorption loss $\mathrm{SE_A}$ instead of the SE. The $\mathrm{SE_A}$ is related to the S-parameters by the following equation:

$$\mathrm{SE}_A = 10\log_{10}\frac{1-|S_{11}|^2}{|S_{21}|^2}. \qquad (4)$$

The EM characterizations of this article are always shown in terms of S-parameters and absorption loss $\mathrm{SE_A}$.

The efficiency of a microwave absorber can be determined by the Rozanov method [31], which is widely used for broadband radar absorption by multilayer. The objective is to obtain the thinnest absorber showing the highest possible absorption. Current radar absorbers are known to have good performance over a narrow frequency band [32], whereas our systems show wideband absorption. The analyzed samples have to be metal backed to fulfill the conditions of applicability of the Rozanov formalism. The Rozanov relation provides an upper limit for the integral of the reflectance R over a given wavelength λ range. The following inequality gives the minimal thickness of a physically achievable radar absorber:

$$\int_{\lambda_i}^{\lambda_f} \ln R(\lambda)d\lambda \leq 2\pi^2 \sum_n(\mu_n d_n) \qquad (5)$$

where μ_n and d_n are static permeability and thickness of each slab, $n \in \mathbb{N}$ [31]. As the configuration prevents any transmittance T, we assume that absorbance $A = 1 - R$. We will use this relevant way to gauge the performance of the absorbers described in this article.

III. Results and Discussion

We have described the fabrication process of Ni-NWs—polymer composite that gives a thin conductive-magnetic mesh sandwiched between polycarbonate layers. This confinement allows an efficient use of the nanofillers since the percolation

TABLE I
SUM UP OF THE IN-PLANE (BY WAVEGUIDE TECHNIQUE) PROPERTIES AVERAGED OVER MEASURED SPECTRUM

	$\varepsilon_r^{'}$	σ [S/m]	μ_s	$\mu_r^{'}$	$\mu_r^{''}$
$0.29\,\mathrm{mg/cm^2}$	3.2 ($\pm$2.7)	0.5 ($\pm$0.2)	n/a	1.1 ($\pm$0.2)	1.4 ($\pm$1.1)
$0.47\,\mathrm{mg/cm^2}$	2.9 ($\pm$1.7)	1.5 ($\pm$0.6)	17	1.8 ($\pm$1.5)	1.5 ($\pm$0.7)
$0.92\,\mathrm{mg/cm^2}$	3.1 ($\pm$0.9)	3.0 ($\pm$2.1)	n/a	2.4 ($\pm$0.8)	1.6 ($\pm$0.6)
$3.26\,\mathrm{mg/cm^2}$	3.2 ($\pm$1.8)	41 ($\pm$22)	146	19 ($\pm$4.0)	13 ($\pm$7.0)

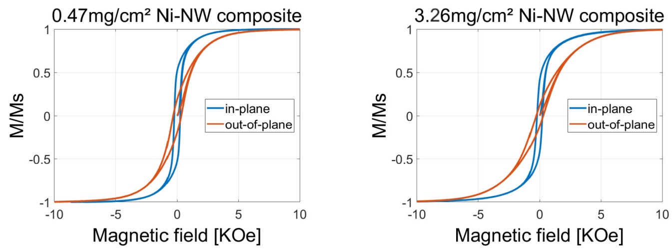

Fig. 2. In-plane and out-of-plane hysteresis loops of composites with 0.47 and 3.26 mg/cm^2 of Ni-NW.

threshold is quickly reached (also helped by the very high aspect ratio of the NWs).

The ferromagnetic properties of the sandwiches have been revealed by AGFM hysteresis loops. Fig. 2 shows the in-plane and out-of-plane characterizations of the sandwiches with 0.47 and 3.26 mg/cm^2 of Ni-NWs. The out-of-plane hysteresis loops are both tilted by comparison with the in-plane ones; this is the proof that these films have a permeability depending on the direction. The strong anisotropy is due to an alignment of the NWs in the plane. The AGFM analysis reveals a magnetic response of the material useful for the Rozanov formalism, but they are not valid to quantify any property since it is depending on frequency [33]. We, hence, proceed next to characterization in the gigahertz range in order to obtain the required parameters for preliminary simulations.

The polycarbonate-nickel nanowire (PC—Ni-NW) multilayered films have been characterized in order to define their complex permittivity and permeability in the microwave range. Complex permittivity contains information about the dielectric constant $\varepsilon_r^{'}$, which is close to pure PC for all composites, and about conductivity σ, which dominated by the imaginary part since $\varepsilon_r = \varepsilon_r^{'} - \frac{i\sigma}{\varepsilon_o \omega}$, where i is the imaginary unit, ε_o is the vacuum dielectric constant, and ω is the pulsation. Permeability is also defined by a complex number $\mu_r = \mu_r^{'} - i\mu_r^{''}$ in frequency. The sandwich with 3.26 mg/cm^2 of Ni-NW is measured by the microstrip and waveguide methods in order to determine its out-of-plane and in-plane properties respectively (see Fig. 3). As expected, Fig. 3 shows that in-plane values of permittivity, conductivity, and permeability are higher than out-of-plane values. The in-plane configuration maximizes the interaction of the EM wave with the mesh of nanofillers because they are oriented in the direction of the electric and magnetic fields. Note that the experimental oscillations are due to a slight impedance mismatch over the swept frequency range. Furthermore, the algorithm for extracting the physical properties from S-parameters inevitably amplifies these oscillations.

Besides the aforementioned example, the composites with different amounts of Ni-NWs have been characterized. It is possible

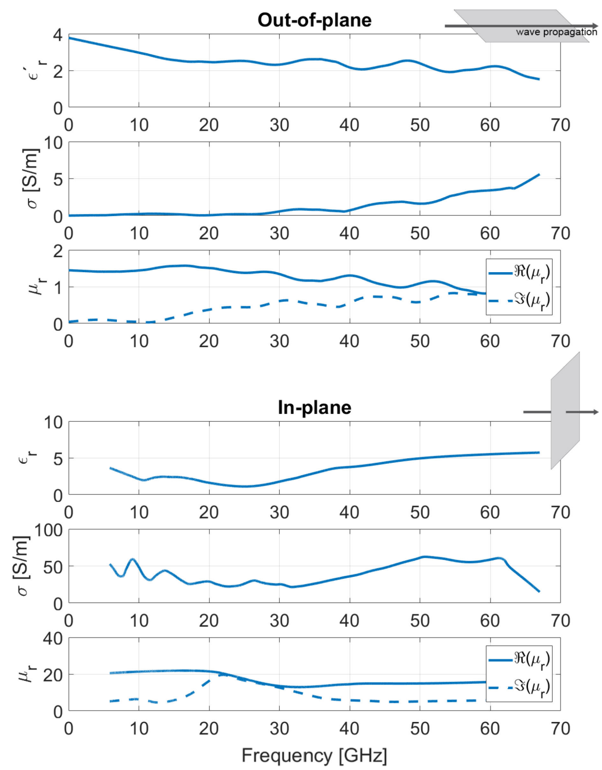

Fig. 3. Out-of-plane and in-plane characterization of a sandwich based on 3.26 mg/cm^2 of Ni-NW deposited on a PC filter and sandwiched between two PC sheets. The insets show the wave propagation.

to obtain a range of values for $\varepsilon_r^{'}$, σ, $\mu_r^{'}$, and $\mu_r^{''}$ depending on the quantity of deposited NWs. Table I gives the averaged value over the spectrum of the in-plane effective properties of the composite films as a function of the mass of Ni-NWs for the fixed surface of 950 mm^2. The maximum variations around the average values are bounded by the values given in brackets. Let us note that we work in a window of the frequency range (8–67 GHz) instead of the half plane of the Kramers–Kronig theory. The imaginary part of permittivity (i.e., conductivity) can then change without a direct influence on the real part on this specific range. We think a short circuiting of the nanofillers (comparable to a circuit of resistances–capacitors) significantly increases the effective conductivity with the concentration of the NWs, while the dielectric constant remains unchanged. The static permeability μ_s comes from the AGFM analysis. The objective is to reach a precise balance between the conductivity and permeability to maximize the absorption loss. The optimum stack follows an exponential distribution of the permittivity and permeability. Furthermore, a stack of only four layers maximize the absorption/thickness ratio for the defined frequency range.

A fine tuning of the quantity of sandwiched NWs leads to a multilayer getting close to optimal absorber. The mathematical approach shows that the imaginary parts of the permittivity and permeability should be high. Yet, this compromise would be difficult to achieve, for instance, with a nanometric surface deposition of nickel because the ferromagnetic influence would be negligible compared to conductivity. Indeed, the bulk conductivity of nickel is highly dominant regarding the low contribution of permeability. The 7 μm-thick entangled Ni-NWs deposited layer decreases drastically the effective conductivity of the nanofiller network because of the presence of electrical contact resistances that reduce conductivity. Furthermore, it is simple to control precisely σ, $\mu_r^{'}$, and $\mu_r^{''}$ via the quantity of nanocharges. This is advantageous here to tailor favorable properties for the multilayered absorbing structure.

The so-made series of conductive-magnetic sandwiches is useful to build absorbing multilayers obtained by stacking such sandwiches. An arrangement in a gradient of conductivity–permeability is the best solution to attenuate progressively the incoming EM waves. The increasingly conductive network absorbs the electric field through the multilayer without significantly reflecting the energy [20]. The same applies for the layer-by-layer increase of permeability that gradually attenuates the magnetic field of the waves. Fig. 4 shows the results of the four-layers absorber built from Ni-NW sandwiches measured in Table I. Because of the intrinsic oscillation of the waveguide method, we show the theoretical prediction in dotted line in the following figures. The Ni-NW multilayer is compared with another four-layer stack (700 μm-thick) made of CNT sandwiches arranged with the same gradient strategy. The method of fabrication of those CNT composites in presented in some detail in [3]. The effective conductivity of each CNT composite layer is equivalent to that of the Ni-NW sandwiches in order to separate the contribution of the sole magnetic component. The two multilayers follow, therefore, the same gradient of the conductivity. Unsurprisingly, the absorption index favors the Ni-NWs-based multilayer. Its total thickness is 600 μm, while the mean absorption index (not shown) over the spectrum is close to 90% or an average absorption loss $\mathrm{SE_A}$ of 18 dB. Fig. 4 shows the S-parameters and the absorption loss for a measurement from port 1 to port 2. The characterization in the reverse way would demonstrate a substantial reflection (the phenomenon is detailed in previous researches [3], [20]). The reflection (S_{11}) and the transmission (S_{21}) are significant for the PC–CNT multilayer, explaining the worse absorption loss. Referring to reflection coefficient [see (2)], the decrease of S_{11} is favored by a characteristic impedance Z_c closer to that of air, meaning that μ_r gets value higher than 1 to compensate the permittivity ε_r of the composite. Likewise, S_{21} is decreased thanks to high $\mu_r^{''}$ and $\varepsilon_r^{''}$ via the transmission coefficient T [see (1)]. Fig. 4, hence, confirms that magnetic NW-based sandwiches combined with a gradient arrangement are very efficient for microwave shielding. The dotted lines are the predictions of the multilayer computed from measured physical parameters of each separated layer directly used as input.

The two four-layer absorbers described previously are characterized following the Rozanov formalism. The multilayers are only measured at port 1 and the backside of the absorbers is coated with an aluminum foil to ensure total reflection. Referring to the Rozanov inequality [see Section II-B, (5)], for the same reflection target, the thickness d_n can be decreased in inverse proportion to μ_n. In practice, we aim to get as close as possible to the theoretical minimum thickness, i.e., the equality in (5). Fig. 5 shows the experimental results (full lines) compared with the simulated prediction (dotted lines). The Ni-NWs-based multilayer exhibits a reflectance 5 dB lower than the CNT multilayer

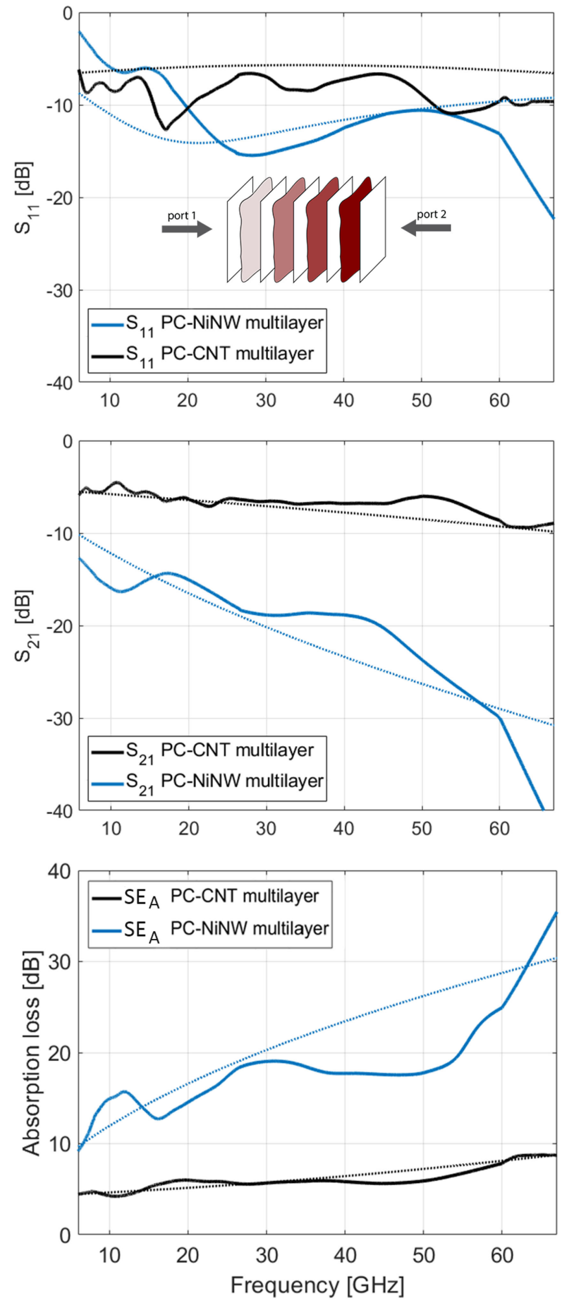

Fig. 4. Comparison between PC–Ni-NW and PC–CNT four-layer structures having same values of complex permittivity and different values of relative permeability. S-parameters show lower reflection S_{11} and transmission S_{21} of the Ni-NW-based absorber than the CNT-based multilayer; the absorption loss follows the same trend. The dotted lines are the theoretical predictions of layer stacks. The inset illustrates the multilayer where white layers are pure PC and red layers are thin nanofiller depositions.

TABLE II
COMPARISON OF ABSORBER PERFORMANCES WITH THE LITERATURE

	description	bandwidth	efficiency	thickness	ref
σ-films	Cu-NW@MWCNTs in PS	8–12.5 GHz	SE=35dB, A=54%	210 µm	[34]
	Metal-NWs in polymer	8–12.5 GHz	SE=20dB	210 µm	[35]
	Sheet of Ag-NWs in cellulose	1 GHz	SE=48.6dB	$154.1\mu m < t < 164.2\mu m$	[36]
	Sheet of Ag-NWs in PDMS	8–12.5 GHz	SE=42dB, $SE_A \simeq$5dB	active surface $< 200nm$	[37]
μ-films	Bucky-paper of CoFeNiBSiMo-MNWs	1–2 GHz	SE=18dB, A=98.4%	640 µm	[6]
	MNWs in PAni	12.4–18 GHz	SE_A=45dB	na	[8]
	Ni-NWs in Al_2O_3 template	2–18 GHz	$SE_R \simeq$1dB	1mm	[13]
			$SE_R \simeq$3dB	2mm	
			$SE_R \simeq$8.5dB	3mm	
			SE_R=8.5dB	3mm	
			$SE_R \simeq$5.5dB	4mm	
			$SE_R \simeq$4.5dB	5mm	
	FeCo-nanorods+MWCNTs in PVDF	8–18 GHz	SE=44dB	5mm	[14]
	Fe_3O_4|MWCNTs core|shell in PVDF	12–18 GHz	SE=44dB, A=77%	600 µm	[16]
	Ni@MWCNTs in PS	2–4 GHz	SE_R=33dB	6mm	[17]
	Fe-filled CNTs	2–18 GHz	SE_R=21.9dB	2mm	[18]
	MWCNTs+NiFe-MNP+BaTi-NP in PC+PVDF	8–18 GHz	SE=44dB, SE_R=15dB, SE_A=25dB	5mm	[38]
	Fe-MNPs in PU	2–18 GHz	MBRL=20dB	1.524mm	[39]
	N-doped Co-MNP @ CNTs	2–18 GHz	SE $\simeq$33dB, $SE_A \simeq$30dB	4mm	[42]
	YIG in PAni-wax	8–18 GHz	SE=44.8dB, SE_A=40.2dB	4mm	[43]
foams	Ag-NWs in foamed PU	8.2-12.5 GHz	SE=64dB, SE_R=10dB, $SE_R \simeq$64dB	2.3mm	[10]
	Ag-NWs @ carbon sponges	8.2-12.5 GHz	SE=70.1dB, $SE_A \simeq$60dB	3mm	[40]
	Graphene in foamed PDMS	8–12 GHz	SE$\simeq$22dB, $SE_R \simeq$3dB, $SE_A \simeq$18dB	1mm	[41]
	MWCNTS in foamed PCL	25–40 GHz	SE$\simeq$80dB, $SE_R \simeq$9dB	2mm	[44]
			SE$\simeq$30dB, $SE_R \simeq$13dB	2mm	
	Graphene in foamed PMMA	8-12 GHz	SE=15dB	2.4mm	[45]
	Graphene in foamed PS	8-12 GHz	SE=29dB	2.5mm	[46]
multilayers	multilayer of MWCNTs in PC	8–67 GHz	A$\simeq$85%	4.9mm	[3]
	sandwich of Fe|Al-Fe alloy|Fe	30 kHz – 1.5 GHz	SE=70–80dB	1mm	[7]
	multilayer of ...|PC|CNTs|...	8–40 GHz	A$\simeq$90%	2.7mm	[20]
	trilayer of CNTs in PCL foam	8–36 GHz	SE=45dB, R$\simeq$20dB	30mm	[27]
	multilayer of ...|PC|Ni-NWs|...	8–67 GHz	SE_A=34.3dB, A=97.4%	600 µm	[here]

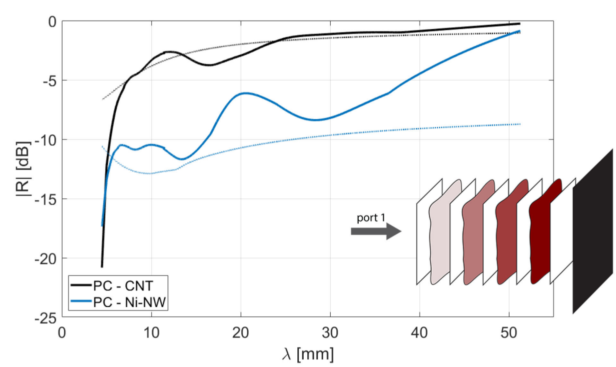

Fig. 5. Characterization following the Rozanov formalism of two multilayers based on CNTs and Ni-NWs. Both structures are composed of 4 PC – Ni-NW or PC – CNT sandwiches whose physical properties are equal except for permeability. The dotted lines are the predictions for each stack. The inset illustrates the multilayer back-covered by a metal foil (in black).

up to a wavelength of 40 mm. This is especially favorable in the Rozanov formalism because the integral on the left-hand side of (5) is taken over a relevant wavelength range. Thanks to the measurement of the reflection coefficient over the considered spectrum, we can calculate the theoretical minimal thickness of the magnetic multilayer. This optimum corresponds to a perfect optimized structure and could be as low as 35 μm instead of the actual 600 μm for the experimental Ni-NW multilayer. The corresponding CNT-based multilayer is closer to the ultimate limit as a nonmagnetic absorber with a theoretical minimum thickness of 205 μm (instead of the actual 700 μm). In the latter case, the managed conductivity gradient is very well adapted. A significant additional optimization of the magnetic film stack is thus possible but it requires a very fine management of the physical properties of each layer.

This evaluation highlights the interest of magnetism for the microwave absorption. First, the global absorption is higher for the Ni-NW multilayer. Furthermore, the Rozanov formalism shows that a fully optimized magnetic multilayer absorber with comparable broadband performance would be about six times thinner than the CNT-based system.

IV. CONCLUSION

We have developed, tested, and analyzed thin and flexible multilayer structures combining a dielectric polymer and ferromagnetic NWs. The metallic NWs are widely used for applications requiring high SE [34], [35]. Ultrathin metal-NW sheets reach impressive SE/thickness ratio, but at the expense of a high reflection resulting a weak absorption loss [36], [37]. Our transmission and reflection are both below -10 dB, which gives a mean absorption loss of 18 dB (or an absorbance of 90%) over a wide microwave frequency range, despite the thickness of 600 μm. The fine control of conductivity and permeability allowed by our approach as well as a smart conductivity/permeability gradient stacking of the layers lead to very high-efficiency absorbers. It results in higher performances compared to homogeneous ferromagnetic nanocomposites [14], [16], [38], [39]. Scientific literature reports similar performances for foam with the inconvenient of thickness [10], [40], [41]. As an indication, Table II shows the performance of some comparable EMI shielding solutions. The factor of merit often varies according to the paper making of any rigorous comparison difficult; however the absorption loss and the thickness of our multilayer demonstrates a competitive efficiency over a wide spectrum. The analysis by the Rozanov formalism gauges the performance compared to the theoretical limit and confirms the great potential of ferromagnetic films in gradient for RF absorption.

Because of their flexibility and low thickness, the multilayers can adapt to almost any shape and so isolate devices from external and internal fields. Realistically, the Ni-NW film absorbers are particularly suited for specific compact devices such as microchips, sensors, or medical probes. The analytic model developed to simulate the structures is in good agreement with the experimental characterization and could further be extended to the design of new systems operating in other frequency ranges.

ACKNOWLEDGMENT

The authors would like to thank D. Spôte, P. Simon, and J. M. Martinez Huerta for magnetic and electromagnetic characterization, F. Glineur, I. Molenberg, F. Abreu Araujo, G. Hamoir, and F. Tao for fruitful discussions, and P. van Velthem, E. Ferain, P. Lipnik, and M. Sclavon for assistance during microscopic observations and chemical analysis.

REFERENCES

[1] N. Violette, *Electromagnetic Compatibility Handbook*. Berlin, Germany: Springer, 2013.
[2] L. H. Hemming, *Architectural Electromagnetic Shielding Handbook: A Design and Specification Guide*. Hoboken, NJ, USA: Wiley, 2000.
[3] Y. Danlée, C. Bailly, and I. Huynen, "Thin and flexible multilayer polymer composite structures for effective control of microwave electromagnetic absorption," *Composites Sci. Technol.*, vol. 100, pp. 182–188, 2014.
[4] J. A. Kong, *Electromagnetic Wave Theory*. Cambridge, MA, USA: EMW, 2000.
[5] P. M. Raj, D. Mishra, H. Sharma, M. Swaminathan, and R. Tummala, "Nanomagnetic materials and structures, and their applications in integrated RF and power modules," in *Nanomagnetism*. Cheshire, U.K.: One Central Press, 2014, ch. 1, pp. 1–29.
[6] F. X. Qin *et al.*, "Exceptional electromagnetic interference shielding properties of ferromagnetic microwires enabled polymer composites," *J. Appl. Phys.*, vol. 108, no. 4, 2010, Art. no. 044510.
[7] X. Ma, Q. Zhang, Z. Luo, X. Lin, and G. Wu, "A novel structure of ferro-aluminum based sandwich composite for magnetic and electromagnetic interference shielding," *Mater. Des.*, vol. 89, pp. 71–77, 2016.
[8] K. Singh, A. Ohlan, A. K. Bakhshi, and S. K. Dhawan, "Synthesis of conducting ferromagnetic nanocomposite with improved microwave absorption properties," *Mater. Chem., Phys.*, vol. 119, no. 1–2, pp. 201–207, 2010.
[9] A. Saib *et al.*, "Carbon nanotube composites for broadband microwave absorbing materials," *IEEE Trans. Microw. Theory Technol.*, vol. 54, no. 6, pp. 2745–2754, Jun. 2006.
[10] Z. Zeng *et al.*, "Ultralight and flexible polyurethane/silver nanowire nanocomposites with unidirectional pores for highly effective electromagnetic shielding," *ACS Appl. Mater. Interfaces*, vol. 9, no. 37, pp. 32 211–32 219, 2017.
[11] J.-M. Thomassin *et al.*, "Multiwalled carbon nanotube/poly (ε-caprolactone) nanocomposites with exceptional electromagnetic interference shielding properties," *J. Phys. Chem. C*, vol. 111, no. 30, pp. 11 186–11 192, 2007.
[12] P. Pötschke, T. Fornes, and D. Paul, "Rheological behavior of multiwalled carbon nanotube/polycarbonate composites," *Polymer*, vol. 43, no. 11, pp. 3247–3255, 2002.
[13] B. Gao, L. Qiao, J. Wang, Q. Liu, F. Li, J. Feng, and D. Xue, "Microwave absorption properties of the Ni nanowires composite," *J. Phys. D, Appl. Phys.*, vol. 41, no. 23, 2008, Art. no. 235005.
[14] I. Arief, S. Biswas, and S. Bose, "Tuning the shape anisotropy and electromagnetic screening ability of ultrahigh magnetic polymer and surfactant-capped FeCo nanorods and nanocubes in soft conducting composites," *ACS Appl. Mater. Interfaces*, vol. 8, no. 39, pp. 26 285–26 297, 2016.
[15] F. Mederos-Henry *et al.*, "Decoration of nanocarbon solids with magnetite nanoparticles: Towards microwave metamaterial absorbers," *J. Mater. Chem. C*, vol. 4, no. 15, pp. 3290–3303, 2016.
[16] Y. Bhattacharjee, D. Chatterjee, and S. Bose, "Core-multishell heterostructure with excellent heat dissipation for electromagnetic interference shielding," *ACS Appl. Mater. Interfaces*, vol. 10, no. 36, pp. 30 762–30 773, 2018.
[17] R. K. Srivastava *et al.*, "Ni filled flexible multi-walled carbon nanotube-polystyrene composite films as efficient microwave absorbers," *Appl. Phys. Lett.*, vol. 99, p. 113–116, 2011.
[18] X. Gui *et al.*, "Optimization of electromagnetic matching of Fe-filled carbon nanotubes/ferrite composites for microwave absorption," *J. Phys. D, Appl. Phys.*, vol. 42, no. 7, 2009, Art. no. 075002.
[19] Y. Bhattacharjee, I. Ariefa, and S. Bose, "Recent trends in multi-layered architectures towards screening electromagnetic radiation: Challenges and perspectives," *J. Mater. Chem. C*, vol. 5, no. 30, pp. 7390–7403, 2017.
[20] Y. Danlée, I. Huynen, and C. Bailly, "Thin smart multilayer microwave absorber based on hybrid structure of polymer and carbon nanotubes," *Appl. Phys. Lett.*, vol. 100, no. 21, 2012, Art. no. 213105.
[21] S. Mrowec and Z. Grzesik, "Oxidation of nickel and transport properties of nickel oxide," *J. Phys. Chem. Solids*, vol. 65, no. 10, pp. 1651–1657, 2004.
[22] A. Fert and L. Piraux, "Magnetic nanowires," *J. Magnetism Magn. Mater.*, vol. 200, no. 1–3, pp. 338–358, 1999.
[23] A. M. Nicolson and G. F. Ross, "Measurement of the intrinsic properties of materials by time-domain techniques," *IEEE Trans. Instrum. Meas.*, vol. IM-19, no. 4, pp. 377–382, Nov. 1970.
[24] W. B. Weir, "Automatic measurement of complex dielectric constant and permeability at microwave frequencies," *Proc. IEEE*, vol. 62, no. 1, pp. 33–36, Jan. 1974.
[25] Z. Szabó, G.-H. Park, R. Hedge, and E.-P. Li, "A unique extraction of metamaterial parameters based on Kramers–Kronig relationship," *IEEE Trans. Microw. Theory Techn.*, vol. 58, no. 10, pp. 2646–2653, Oct. 2010.
[26] N. Quiévy *et al.*, "Electromagnetic absorption properties of carbon nanotube nanocomposite foam filling honeycomb waveguide structures," *IEEE Trans. Electromagn. Compat.*, vol. 54, no. 1, pp. 43–51, Feb. 2012.
[27] J.-M. Thomassin, C. Jérôme, T. Pardoen, C. Bailly, I. Huynen, and C. Detrembleur, "Polymer/carbon based composites as electromagnetic interference (EMI) shielding materials," *Mater. Sci. Eng., R, Rep.*, vol. 74, no. 7, pp. 211–232, 2013.
[28] Y. Danlée, C. Bailly, and I. Huynen, "Frequency-selective coatings based on EBG structure combining carbon nanotubes with polymeric or ceramic substrate," in *Proc. 8th Eur. Conf. Antennas Propag.*, 2004, pp. 2500–2503.
[29] T. Williams, *EMC for Product Designers*, 5th ed. Newton, MA, USA: Newnes, 2017.
[30] J. Tahalyani, K. K. Rahangdale, R. Aepuru, B. Kandasubramanian, and S. Datar, "Dielectric investigation of a conducting fibrous nonwoven porous mat fabricated by a one-step facile electrospinning process," *RSC Adv.*, vol. 6, no. 43, pp. 36 588–36 598, 2016.
[31] K. N. Rozanov, "Ultimate thickness to bandwidth ratio of radar absorbers," *IEEE Trans. Antennas Propag.*, vol. 48, no. 8, pp. 1230–1234, Aug. 2000.
[32] H. Li, L. H. Yuan, B. Zhou, X. P. Shen, Q. Cheng, and T. J. Cui, "Ultrathin multiband gigahertz metamaterial absorbers," *J. Appl. Phys.*, vol. 110, no. 1, 2011, Art. no. 014909.
[33] K. N. Rozanov, M. Y. Koledintseva, and E. P. Yelsukov, "Frequency-dependent effective material parameters of composites as a function of inclusion shape," in *Composites and Their Properties*, N. Hu, Ed. Croatia: Intech, 2012.
[34] M. Al-Saleh, G. Gelves, and U. Sundararaj, "Copper nanowire/polystyrene nanocomposites: Lower percolation threshold and higher EMI shielding," *Composites A, Appl. Sci. Manuf.*, vol. 42, no. 1, pp. 92–97, 2011.
[35] G. Gelves, M. Al-Saleh, and U. Sundararaj, "Highly electrically conductive and high performance EMI shielding nanowire/polymer nanocomposites by miscible mixing and precipitation," *J. Mater. Chem.*, vol. 21, no. 3, pp. 829–836, 2011.
[36] T.-W. Lee, S.-E. Lee, and Y. G. Jeong, "Highly effective electromagnetic interference shielding materials based on silver nanowire/cellulose papers," *ACS Appl. Mater. Interfaces*, vol. 8, no. 20, pp. 13 123–13 132, 2016.

[37] J. Jung *et al.*, "Highly stretchable and transparent electromagnetic interference shielding film based on silver nanowire percolation network for wearable electronics applications," *ACS Appl. Mater. Interfaces*, vol. 9, no. 51, pp. 44 609–44 616, 2017.

[38] S. Biswas, G. P. Kar, and S. Bose, "Engineering nanostructured polymer blends with controlled nanoparticle location for excellent microwave absorption: A compartmentalized approach," *Nanoscale*, vol. 7, no. 26, pp. 11 334–11 351, 2015.

[39] Z. Guo, S. Park, and T. Hahn, "Magnetic and electromagnetic evaluation of the magnetic nanoparticle filled polyurethane nanocomposites," *J. Appl. Phys.*, vol. 101, no. 9, 2007, Art. no. 09M511.

[40] Y. Wan, P. Zhu, Shu Hui, R. Sun, C. Wong, and W. Liao, "Anticorrosive, ultralight, and flexible carbon-wrapped metallic nanowire hybrid sponges for highly efficient electromagnetic interference shielding," *Small*, vol. 14, no. 27, 2018, Art. no. 1800534.

[41] Z. Chen, C. Xu, C. Ma, W. Ren, and H. Cheng, "Lightweight and flexible graphene foam composites for highperformance electromagnetic interference shielding," *Adv. Mater.*, vol. 25, no. 9, pp. 1296–1300, 2013.

[42] R. Kumar *et al.*, "Nitrogen doping as a fundamental way to enhance the EMI shielding behavior of cobalt particle-embedded carbonaceous nanostructures," *New J. Chem.*, vol. 43, no. 14, pp. 5568–5580, 2019.

[43] H. K. Choudhary, R. Kumar, S. P. Pawar, A. V. Anupama, S. Bose, and B. Sahoo, "Effect of coral-shaped yttrium iron garnet particles on the EMI shielding behaviour of yttrium iron garnet-polyaniline-wax composites," *Chem. Sel.*, vol. 3, no. 7, pp. 2120–2130, 2018.

[44] J.-M. Thomassin, C. Pagnoulle, L. Bednarz, I. Huynen, R. Jérôme, and C. Detrembleur, "Foams of polycaprolactone/MWNT nanocomposites for efficient EMI reduction," *J. Mater. Chem.*, vol. 18, no. 7, pp. 792–796, 2008.

[45] H.-B. Zhang, Q. Yan, W.-G. Zheng, Z. He, and Z.-Z. Yu, "Tough graphene-polymer microcellular foams for electromagnetic interference shielding," *ACS Appl. Mater. Interfaces*, vol. 3, no. 3, pp. 918–924, 2011.

[46] D.-X. Yan, P.-G. Ren, H. Pang, Q. Fu, M.-B. Yanga, and Z.-M. Li, "Efficient electromagnetic interference shielding of lightweight graphene/polystyrene composite," *J. Mater. Chem.*, vol. 22, no. 36, pp. 18 772–18 774, 2012.

Yann Danlée received the Ph.D. degree in applied sciences from the Université catholique de Louvain (UCLouvain), Louvain-la-Neuve, Belgium, in 2015. His Ph.D. study was focused on metamaterials able to absorb, polarize, or deflect the electromagnetic waves.

He is currently the CTO of VOCSens, Louvain-la-Neuve, Belgium, responsible for the R&D of gas microsensors and RF telecommunication. His research interests include structured nanocomposites controlling the microwave propagation.

Christian Bailly received the Ph.D. degree in applied sciences from the Université catholique de Louvain (UCLouvain), Louvain-la-Neuve, Belgium, in 1993.

He is currently a Full Professor with the School of Engineering, UCLouvain. His research activities with the Bio and Soft Matter Research Division, Institute of Condensed Matter and Nanosciences, UCLouvain, focus on the structure-property relationships of polymer-based systems, including blends and nanocomposites. His current research interests include the quantitative prediction of rheological properties from structural knowledge.

Isabelle Huynen (M'96–SM'06) received the Ph.D. degree in applied sciences from the Université catholique de Louvain (UCLouvain), Louvain-la-Neuve, Belgium, in 1994.

Since 1999, she has been with the National Fund for Scientific Research (FRS-FRNS), Bruxelles, Belgium, where she is currently the Research Director, and is a part-time Professor with UCLouvain. Her current research interests include nanotechnology, nanodevices, and nanomaterials for microwave and millimeter wave applications, including metamaterials, antennas, and absorbers.

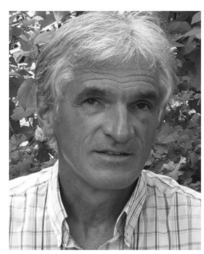

Luc Piraux received the Ph.D. degree from the University of Louvain, Louvan-la-Neuve, Belgium, in 1987.

He was a Research Associate with the National Fund for Scientific Research, Bruxelles, Belgium, during 1989–2001. He is currently with the Institute of Condensed Matter and Nanosciences, Université catholique de Louvain, where his research activities include basic experimental research in the field of nanostructured materials and low-dimensional systems. His research team has expertise in the fabrication of magnetic and superconducting nanowires as well as in the fabrication of highly ordered nanoporous alumina templates. He has authored and coauthored more than 200 publications in peer-reviewed journals and holds three patents. His current research interests include the field of spintronics, nanomagnetism, low-dimensional superconductivity, vortex dynamics, and development of microwave devices.